

NATIONAL AERONAUTICS AND SPACE ADMINISTRATION

Technical Report 32-1545

*DEXTER—A One-Dimensional Code for Calculating
Thermionic Performance of Long Converters*

C. D. Sawyer

**CASE FILE
COPY**

**JET PROPULSION LABORATORY
CALIFORNIA INSTITUTE OF TECHNOLOGY
PASADENA, CALIFORNIA**

November 15, 1971

NATIONAL AERONAUTICS AND SPACE ADMINISTRATION

Technical Report 32-1545

*DEXTER—A One-Dimensional Code for Calculating
Thermionic Performance of Long Converters*

C. D. Sawyer

**JET PROPULSION LABORATORY
CALIFORNIA INSTITUTE OF TECHNOLOGY
PASADENA, CALIFORNIA**

November 15, 1971

Preface

The work described in this report was performed by the Propulsion Division of the Jet Propulsion Laboratory.

281-3100-111 11-11-11 11:11:11

Contents

I. Introduction	1
II. Problem Definition	1
A. Fuel Element Description	1
B. Physical Model	1
C. Electrical Model	3
III. Program Description	5
A. Method of Solution	5
B. Capabilities and Restrictions	6
IV. Examples	7
A. Variation of Lead Geometry	7
B. Variation of Lead Arrangement	7
C. Collector Temperature Effects	8
D. Central Short	8
V. User's Manual	10
VI. Error Messages	10
Nomenclature	12
References	13

Tables

1. Data table available in DEXTER	7
2. Net performance of shorted converter	10
3. Input data for DEXTER	10
4. Error messages in DEXTER	11

Figures

1. Typical external-fueled converter design	2
2. Analytic converter model	2
3. Converter electrical model for normal operation	3
4. Converter electric short model	4
5. Converter electric model for internal short	4
6. Converter electric model for emitter-emitter short	4

Contents (contd)

Figures (contd)

7. Converter electrical model for collector–collector short	5
8. Temperature, current and voltage profiles	7
9. Effect of lead geometry on converter output	7
10. Performance of 12.7-cm parallel electron flow converter	8
11. Voltage and temperature profile for liquid metal cooled converter	8
12. Coolant and collector temperature profile for liquid metal cooled converter	8
13. Effect of central short on converter temperature profile	9
14. Effect of central short on converter voltage profile	9
15. Effect of varying short conditions on converter temperature profile	9
16. Effect of varying short conditions on converter voltage profile	9

Abstract

This report describes a versatile code for computing the coupled thermionic electric-thermal performance of long thermionic converters in which the temperature and voltage variations cannot be neglected. The code is capable of accounting for a variety of external electrical connection schemes, coolant flow paths and converter failures by partial shorting. Example problem solutions are included along with a user's manual.

DEXTER—A One-Dimensional Code for Calculating Thermionic Performance of Long Converters

I. Introduction

An early version of a one-dimensional thermionic performance code has been previously described (Ref. 1). This early version was, however, limited in scope to a specific converter geometry operating under nominal full power conditions and with the converter collector temperature fixed. A new code, DEXTER, replaces the earlier version and is much more flexible in scope. DEXTER allows a variety of boundary conditions to account for

- (1) Counter current or parallel electron flow.
- (2) Collector temperature variations.
- (3) Converter failures by partial shorting.

In addition, the physical properties are allowed a linear temperature dependence. Since the running time is approximately 30 s per case on a UNIVAC 1108 for a 13-cm-long converter, restart capability is built in to allow recovery from computer error or to observe the progress of the convergence. A sample problem is built into the code, so that the user, with FORTRAN NAMELIST input need only enter a minimal amount of data to execute a problem.

II. Problem Definition

A. Fuel Element Description

Due to the one-dimensional nature of the model in this code, it is possible to study a variety of converter geometries, including both internal- and external-fueled. In describing the code, however, attention has been focused on the external-fueled converter.

Current designs of external-fueled thermionic converters are typified by Fig. 1. Nuclear fuel supplies the heat to drive the emitter. Electron emission aids in cooling the emitter, and electrons are collected at the collector. Waste heat is removed by means of liquid metal or heat pipe cooling of the collector. At one or both ends of the converter there is an emitter lead to carry electrons from the external circuit back into the emitter.

B. Physical Model

The converter is approximated one-dimensionally by an annular emitter-collector arrangement as shown in Fig. 2. The fuel-emitter body is replaced by specifying the emitter heat input as a function of distance. In the fuel element described above, the emitter fins and outer fuel

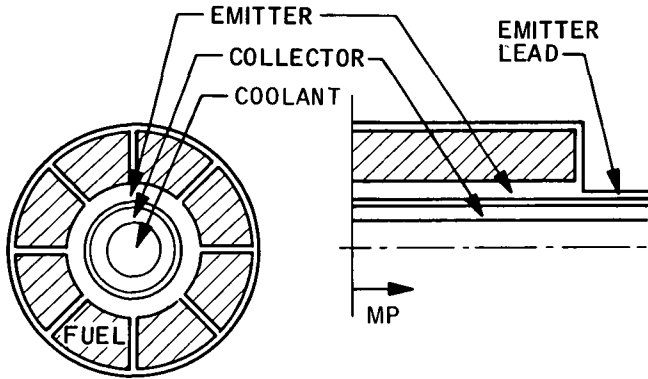


Fig. 1. Typical external-fueled converter design

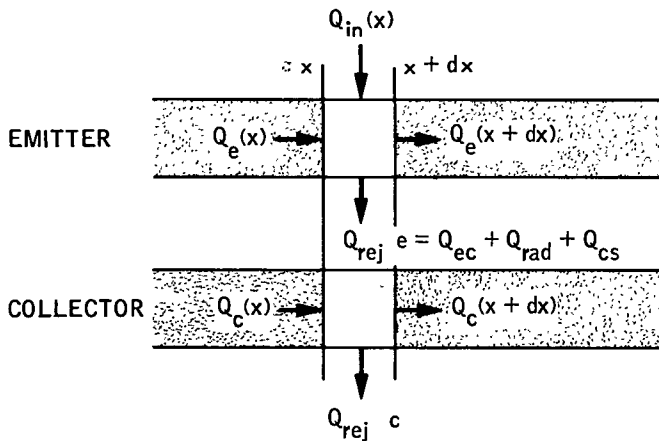


Fig. 2. Analytic converter model

cladding also can conduct heat and electricity to the ends of the converter. Provision is made for this in the analytic model by providing different effective emitter cross-sectional areas for heat and electron conduction. Axial fuel heat conduction is neglected, a good approximation for most ceramic fuels such as UO_2 .

The equations describing the heat transfer processes in the converter can thus be written as (refer to nomenclature for definitions):

$$\frac{dQ_e(x)}{dx} = C_e(Q_{in}(x) - Q_{ec}(j, T_e, T_c, T_{cs}) - Q_{rad}(T_e, T_c) - Q_{cs}(T_e, T_c, T_{cs})) + i_e^2(x) \frac{\rho_e(T_e)}{A_{e1}} \quad (1)$$

$$\frac{dT_e(x)}{dx} = -\frac{Q_e(x)}{A_{e2} k_e(T_e)} \quad (2)$$

$$\frac{dQ_c(x)}{dx} = C_e(Q_{ec}(j, T_e, T_c, T_{cs}) + Q_{rad}(T_e, T_c) + Q_{cs}(T_e, T_c, T_{cs}) - jv(x) + i_c^2(x) \frac{\rho_c(T_c)}{A_c} - C_c h [T_c(x) - T_{co}(x)]) \quad (3)$$

$$\frac{dT_c(x)}{dx} = -\frac{Q_c(x)}{A_c k_c(T_c)} \quad (4)$$

$$\frac{dT_{co}(x)}{dx} = \frac{C_c h}{wC_p} [T_c(x) - T_{co}(x)] \quad (5)$$

The radiation term is determined from a simplified but quite accurate formula (Ref. 2):

$$Q_{rad} = \sigma(\epsilon_e T_e^4 - \epsilon_c T_c^4) \quad (6)$$

$$\frac{1}{\epsilon_e} = \frac{1}{\epsilon_e(T_e)} + \frac{1}{\epsilon_c(\sqrt{T_e T_c})} - 1 \quad (7)$$

$$\frac{1}{\epsilon_c} = \frac{1}{\epsilon_e(\sqrt{T_e T_c})} + \frac{1}{\epsilon_c(T_c)} - 1 \quad (8)$$

The cesium conduction term is given by the Kitrilakis-Meeker formula (Ref. 3)

$$Q_{cs} = 1.1 \times 10^{-6} \frac{(T_e^{1.5} - T_c^{1.5})}{d + 1.15 \times 10^{-5} \frac{(T_e + T_c)}{P_g}} \quad (9)$$

$$P_g = \frac{2.45 \times 10^8}{\sqrt{T_{cs}}} \exp\left(-\frac{8910}{T_{cs}}\right) \quad (10)$$

The collector-coolant heat transfer coefficient is taken from a simplified correlation (Ref. 4)

$$h = \frac{7 k_{co}}{D_{co}} \quad (11)$$

Experience has shown that even for collectors approaching 0.3-cm thickness, it is a good approximation to neglect axial conduction in the collector. This simplifies Eqs. (3-5) to

$$\frac{dT_{co}(x)}{dx} = \frac{1}{wC_p} \left[C_e(Q_{ec} + Q_{rad} + Q_{cs} - jv) + i_c^2 \frac{\rho_c}{A_c} \right] \quad (12)$$

$$T_c = T_{co} + \frac{1}{C_c h} \left[C_e (Q_{ec} + Q_{rad} + Q_{cs} - jv) + i_e^2 \frac{\rho_c}{A_c} \right] \quad (13)$$

An additional simplification in the case of heat pipe cooling can be made, namely,

$$T_c = \text{constant} \quad (14)$$

The left boundary conditions to be applied to Eqs. (1, 2) and (12, 13) are

$$\left. \begin{aligned} Q_e(0) &= 0 \\ T_e(0) &= T_{eo} \\ T_{co}(0) &= T_{coo} \end{aligned} \right\} \quad (15)$$

The emitter lead design forms an important part of the overall performance optimization of the converter. This is because conduction heat losses down the lead are inversely proportional to the lead length-to-area ratio, while lead electrical losses are directly proportional to the same quantity. In many designs the problem of optimization is made complex by the additional ability of the lead to radiate to the collector. Lead conduction losses are given by

$$Q_e(l) = k_L \frac{[T_e(l) - T_c(l)]}{\lambda} - \rho_L \frac{i_e^2 \lambda}{2} \quad (16)$$

In an attempt to compensate for radiative losses, within the spirit of the one-dimensional approach, the second term of Eq. (16) is not included in the model used for DEXTER. In addition, one can show that if lead conductivity k_L varies linearly with temperature, the appropriate temperature for evaluating this property is the mean lead temperature. Therefore, Eq. (16) becomes

$$\lambda = k_L(T_L) \frac{[T_e(l) - T_c(l)]}{Q_e(l)} \quad (17)$$

This equation forms the normal right boundary condition.

For certain cases involving converter shorts, described in more detail below, the short is characterized by a thermal conductivity. In these cases Eq. (17) can be solved for k or k/λ to determine the appropriate right boundary condition.

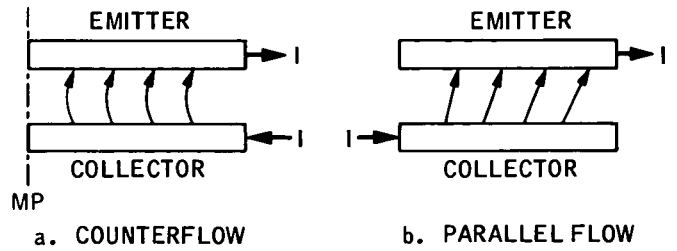


Fig. 3. Converter electrical model for normal operation

C. Electrical Model

1. Normal operation. Two possible converter electron flow patterns are considered within DEXTER: counterflow and parallel flow, indicated schematically in Fig. 3. In the counterflow case the total current appears at the emitter and collector leads on the same end of the converter. At every position within the converter the emitter and collector currents are identical and of opposite sign, decreasing to zero current flow at the converter center. The voltage and current relations are given by

$$\frac{dv(x)}{dx} = - \left[\frac{\rho_e(T_e)}{A_{e1}} + \frac{\rho_c(T_c)}{A_c} \right] i_e(x) \quad (18)$$

$$\frac{di_e(x)}{dx} = C_e j(v, T_e, T_c, T_{cs}) \quad (19)$$

$$i_c(x) = -i_e(x) \quad (20)$$

The left boundary condition is

$$i_e(0) = 0 \quad (21)$$

The net power and voltage obtained at the end of the emitter lead is

$$P_{net} = i_e(l) v_{net} \quad (22)$$

$$v_{net} = v(l) - i_e^2(l) \rho_L \lambda \quad (23)$$

In the parallel flow case, the emitter and collector leads are on opposite ends of the converter. The appropriate relations are

$$\frac{dv(x)}{dx} = - \frac{\rho_e(T_e)}{A_{e1}} i_e(x) - \frac{\rho_c(T_c)}{A_c} i_c(x) \quad (24)$$

$$\frac{di_e(x)}{dx} = C_e j(v, T_e, T_c, T_{cs}) \quad (25)$$

$$i_c(x) = I - i_e(x) \quad (26)$$

with the same left boundary, Eq. (21), and the additional restriction that

$$i_e(l) = I \quad (27)$$

2. Abnormal operation—converter shorts. A generalized circuit diagram involving two series-connected fuel elements with the possibility of internal shorting and emitter-emitter and collector-collector shorting is shown in Fig. 4 (only one-half of each converter is shown for a two-ended counterflow converter, which is assumed for the base case). Here the shorts are all represented by means of electrical resistances located at arbitrary positions along the converter. The interconnection between converters is assigned a lead resistance R_L .

For an internal short resistance R_s , only one complete converter need be examined, provided that the change in effective load resistance seen by the converter can be specified from a data map obtained for normal performance converters. The electron flow pattern is indicated schematically on Fig. 5. There are, in general, four regions of interest in the analysis. The two outermost regions, a and d , can be treated as counterflow converters, with length as a parameter to be determined. Depending on

the overall converter connection pattern, I_L and I_R or the voltages v_L and v_R may be known, or a combination of the two such as

$$v_L = I_L R_L \quad (28)$$

may be known. Regions b and c are also counterflow converters of length to be determined with the right boundary being

$$I_b(l) + I_c(l) = I_s \quad (29)$$

$$v_b(l) = v_c(l) = I_s R_s \quad (30)$$

The thermal equations also require that $T_e(0)$ and $Q_e(0)$ be parameterized.¹

For an emitter-emitter short resistance R_{es} , two complete converters must, in general, be studied. Figure 6 shows the breakdown of the problem into six regions, of which a , d , e , and f are counterflow and b and c are parallel flow. The necessary boundary conditions may be derived with the aid of the figure. Again, region length $T_e(0)$ and $Q_e(0)$ must be parameterized in effecting a solution. Note that regions e and f are just the counterflow converter with excess current flowing in the emitter.

Finally, the analytical model for a collector-collector short is shown in Fig. 7. For an external-fueled converter, this short cannot take place except through the coolant channels or leads external to the converter, but the case is shown in generality for other possible converter configurations in which such a short is possible.

¹An equivalent solution method is to define the length of each section based on the location of the temperature maximum and have a non-zero current at that location.

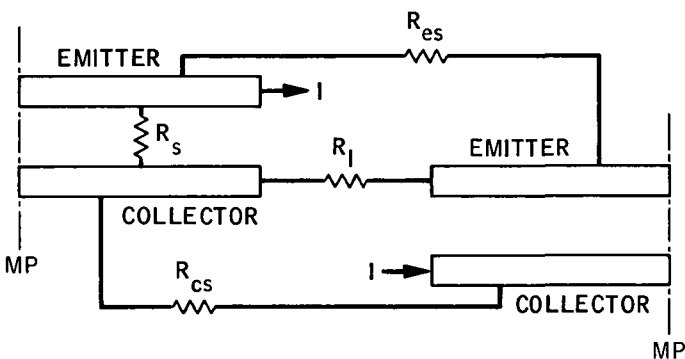


Fig. 4. Converter electric short model

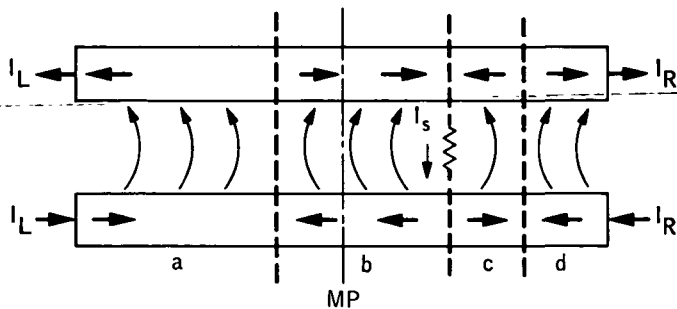


Fig. 5. Converter electric model for internal short

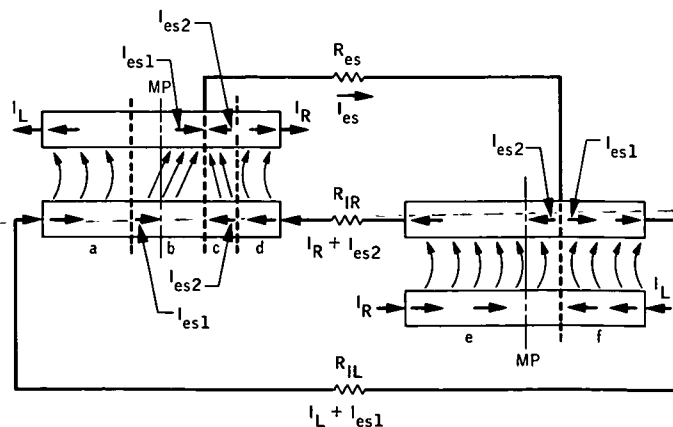


Fig. 6. Converter electric model for emitter-emitter short

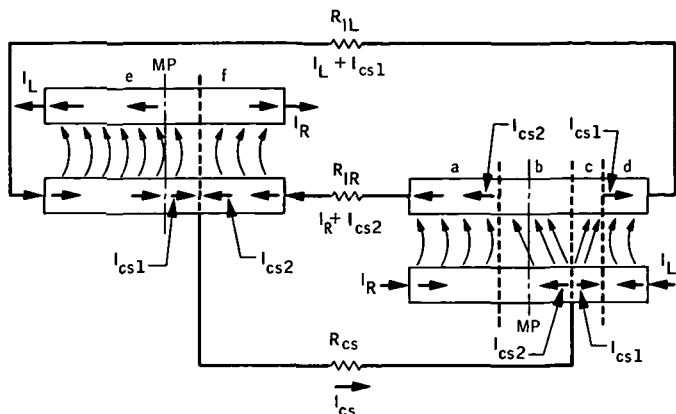


Fig. 7. Converter electrical model for collector-collector short

III. Program Description

A. Method of Solution

1. *Counterflow converter with constant collector temperature.* To show the nature of the solution process, attention will be first given to the counterflow converter with constant collector temperature. The equations to be solved are

$$\frac{dQ_e}{dx} = C_e (Q_{in} - Q_{ec} - Q_{rad} - Q_{cs}) + (i_e + I_{es})^2 \frac{\rho_e}{A_{e1}} \quad (31)$$

$$\frac{dT_e}{dx} = - \frac{Q_e}{A_{e2} k_e} \quad (32)$$

$$\frac{dv}{dx} = - \left(\frac{\rho_e}{A_{e1}} + \frac{\rho_c}{A_c} \right) i_e \quad (33)$$

$$\frac{di_e}{dx} = C_e j \quad (34)$$

where I_{es} is excess (short) emitter current, if any, and the dependence of the variables is not shown. Boundary conditions are

$$\left. \begin{aligned} Q_e(0) &= 0 \\ T_e(0) &= T_{e0} \\ i_e(0) &= 0 \\ k_L \frac{T_e(l) - T_c}{Q_e(l)} &= \lambda \end{aligned} \right\} \quad (35)$$

In order to solve these equations it is necessary to be able to determine Q_{ec} and j at each location. A data map of Q_{ec} vs j and v vs j for a variety of emitter temperatures, collector parameters and cesium reservoir temperatures is available from the SIMCON code (Ref. 5). The v - j data are single-valued if j is the independent variable, but not always single-valued if v is the independent variable, which is the case above. Thus the data were modified at the expense of accuracy in the lower-temperature extinguished mode regime so as to force a single-valued $j(v)$. Also the data were extrapolated to $T_e = T_c$ in order to study converter shorting. The extrapolations were rough in some cases, but fortunately there is very little electron cooling at these low temperatures so that the effect of errors in the extrapolation will be minor. Because it is far simpler to determine a uniform grid if j is the independent variable, an iterative process is required at each location. Thus, knowing T_e , T_c and T_{cs} , a table lookup can be performed for a given j to find v . A modified Newton-Raphson iteration process is used to find that $j(x)$ which corresponds to a known $v(x)$. Then $Q_{ec}(x)$ is also known.

In solving Eqs. (31-35) one of the boundary conditions is known only at the right boundary, so a shooting technique is required. An initial value of $v(0)$ is estimated and then varied until the desired right boundary condition is satisfied. A good estimator for the first guess, $v^0(0)$, can be obtained by assuming that

$$Q_{in}(0) = Q_{ec}(0) + Q_{rad}(0) + Q_{cs}(0) \quad (36)$$

Thus $j(0)$ is iterated until Eq. (36) is satisfied. A fourth-order Runge-Kutta method with automated step-size selection was used to perform the integration.

It turns out that the trajectories obtained [particularly $T_e(x)$] are quite sensitive to the choice of $v(0)$, requiring a knowledge of the order of five or six decimal places to get a meaningful solution. In order to handle this problem, a logarithmic algorithm is first used to get values of $v(0)$ in the correct decade. In this algorithm, upper and lower bounds are estimated for $v(0)$ and modified according to whether the temperature trajectory goes to ∞ or $-\infty$. After modification of the appropriate limit [reducing $v(0)$ causes the T_e temperature trajectory to head toward $+\infty$], the new estimate of $v(0)$ is obtained from

$$v(0)^{j+1} = \frac{v_u^j + v_l^j}{2} \quad (37)$$

In this manner it is usually possible to obtain meaningful $T_e(l)$ values after about 10 iterations.

It is possible to continue iterating with Eq. (37) until the required right boundary condition is satisfied. However, the lead length-to-area ratio is usually desired as a parameter in the output in order to obtain an optimum fuel element design. By trial and error, it was determined that once three meaningful trajectories are obtained by using Eq. (37) it is possible to fit the results by

$$v(0, \lambda) = a + \frac{b}{\lambda - c} \quad (38)$$

and use relation (38) to fill out a parametric performance map for varying values of λ .

2. Parallel flow convertér with constant collector temperature. The parallel flow case replaces Eq. (33) with

$$\frac{dv}{dx} = -\frac{\rho_e}{A_{e1}} i_e - \frac{\rho_c}{A_c} i_c \quad (39)$$

$$i_c = i_e(l) - i_e \quad (40)$$

It is possible to solve this new set of equations exactly as in the counterflow case. However, since $i_e(l)$ is unknown, several solutions are required with $i_e(l)$ treated as a parameter until the estimated value of $i_e(l)$ equals the value obtained by integration. At this time, this additional iteration is not automated in DEXTER, so the user must provide the iterations with overlay cases, each time specifying a new value of $i_e(l)$ as input. Because of the running time of DEXTER, this was done so as to allow maximum ingenuity on the part of the user in obtaining a minimum cost solution.

3. Counterflow converter with varying collector temperature. For this case, additional relations are added to Eqs. (31-35):

$$Q_{rej} = C_e(Q_{ec} + Q_{rad} + Q_{cs} - jv) + (i_e + I_{cs})^2 \frac{\rho_c}{A_c} \quad (41)$$

$$\frac{dT_{co}}{dx} = \frac{Q_{rej}}{wC_p} \quad (42)$$

$$T_c = T_{co} + \frac{Q_{rej}}{C_c h} \quad (43)$$

$$T_{co}(0) = T_{co_0} \quad (44)$$

where I_{cs} is excess (short) current flowing through the collector, if any. Since the thermionic properties Q_{ec} and j also depend on T_c , it would appear that additional iteration is required at each location in order to determine T_c . However, since the thermionic properties are not strongly dependent on T_c , it was decided to update T_c after each integration step to avoid the iteration. $T_c(0)$ is determined from one iteration of the equations at $x = 0$ to determine $Q_{rej}(0)$.

The solution procedure is described here for a double-ended converter, since in this case the solution is no longer symmetric about the converter midplane. It was found that a convenient way to obtain a solution involves solving two counterflow converter problems, one with positive and one with negative flow rate. In matching the solutions it was found that there is a nonzero i_e at the location of the emitter temperature maximum; i.e., the voltage and emitter temperature do not peak at the same place. Thus $i_e(0)$ is given to one converter, $-i_e(0)$ to the other, and the level is adjusted so as to match $v(0)$ and $i_e(0)$ at the point of joining the two "half" converters. In the case of a double-ended converter it is desirable to have identical electrical voltage from either end in order to provide a good voltage match at the reactor bus. Therefore, it is additionally necessary to treat the boundary between the two "half" converters as a parameter; i.e., the length of each side must vary while satisfying the constraint that the total length is a constant. Thus parametric information must be obtained both for $i_e(0)$ and the length of each section. Once again, this procedure has not been automated into the present version of DEXTER so as to allow human ingenuity to minimize the investment in machine time for a complete solution.

4. Abnormally operating converters. The techniques described above provide sufficient flexibility to cover any of the shorted converter situations. No automated solution is programmed into the present version of DEXTER. An example of the solution of a converter central emitter-collector short is given in Section IV-D.

B. Capabilities and Restrictions

Once the set of equations and boundary conditions is fully understood by the user, his ingenuity may discover ways to apply DEXTER to situations not explicitly considered in the original formulation of the problem. For instance, the author has found that DEXTER can be used in conjunction with a fuel redistribution analysis code to solve the problem of fuel movement to form an isothermal

internal cavity. In this problem $Q_{in}(x)$ is not known and must be determined by iteration.

The present version uses a thermionic data table formulated by the SIMCON code for a specific diode performance characteristic. The user may desire to provide his own data tables. If so, it is recommended that the user also replace subroutines TABLE and BOUNDS, which were written for the interpolation of a specific data arrangement. The table lookup is up to four-dimensional but has built into it reductions to lower dimensions in the event that the collector temperature or cesium reservoir temperature exactly matches one of the tabulated sets in the data map. The tabulated data are arranged as shown in Table 1 for each of four collector temperatures: 850, 1000, 1150 and 1300 K. For each T_c , T_e and T_{cs} , there are 15 current density values: 0, 0.5, 1.0, 2.0, 3.0, 4.0, 6.0, 8.0, 10.0, 12.0, 15.0, 20.0, 25.0, 30.0, and 35.0 A/cm². For initial performance scoping it is highly recommended that the tabulated values of T_c and T_{cs} be selected so as to reduce table lookup time. Any attempt to request data outside the table, e.g., $T_{cs} = 650$ K for $T_e = 2000$ K, will be rejected by the code.

Table 1. Data table available in DEXTER
($d = 0.0254$ cm)

T_e , K	T_{cs} , K
1400	540-620 steps of 10 K
1500	540-620
1600	540-620
1700	540-620
1800	540-630
1900	540-640
2000	560-640
2100	580-640
2200	590-640
2300	600-640
2400	600-640

IV. Examples

Physical property and geometric data used on all example cases to be reported here are the built-in values for the code (see Section V). Variable names correspond to those listed in Section V.

A. Variation of Lead Geometry

For this example the collector temperature is fixed at 1000 K. The converter is assumed to be symmetric about the midplane and electron flow is countercurrent. Emitter

temperature, current density and voltage profiles along the converter are shown in Fig. 8 for a typical near-optimum lead geometry. These profile shapes are representative of the types of shapes to be expected in long converters. Note that very little electric power is generated in the last 2 cm of the converter (near the lead). Figure 9 shows how the net electric output and net voltage vary with lead geometry.

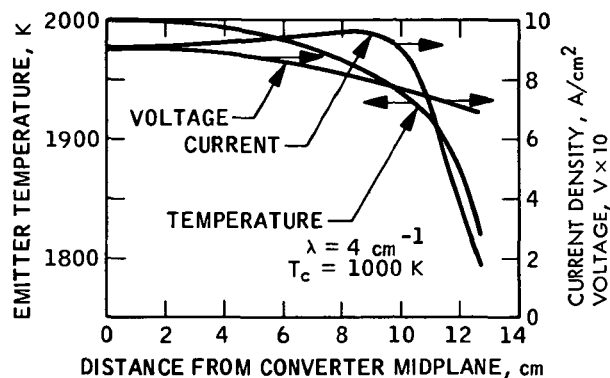


Fig. 8. Temperature, current and voltage profiles

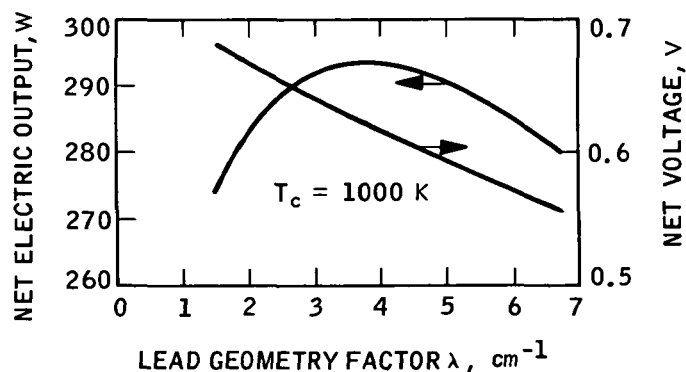


Fig. 9. Effect of lead geometry on converter output

B. Variation of Lead Arrangement

In this example the performance of a converter of 12.7-cm length with emitter and collector leads at opposite leads of the converter (parallel electron flow) is computed. The solution of the parallel electron flow case involves an iteration on total current flow (see Eq. 27). Thus performance data were run assuming $i_c(0) = 400, 450$ and 500 A (Fig. 10). The solution line is the locus of $i_c(12.7 \text{ cm}) = i_c(0)$. This line then was used to interpolate the solution for net power, also shown in Fig. 10.

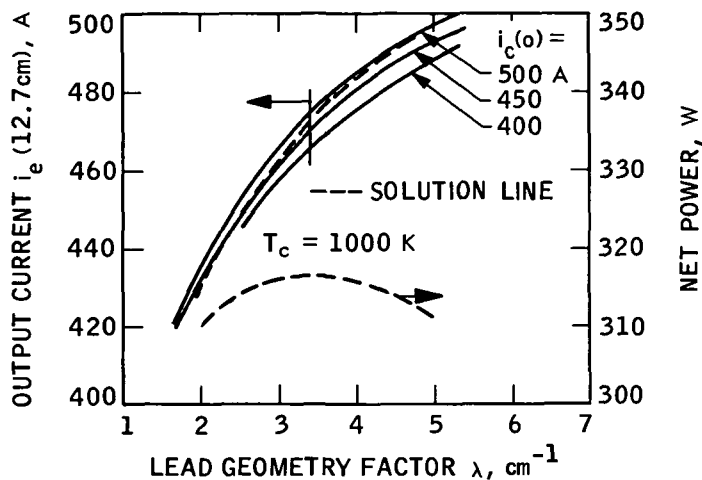


Fig. 10. Performance of 12.7-cm parallel electron flow converter

C. Collector Temperature Effects

In this example, the converter studied was 25.4 cm long with electric leads at both ends (countercurrent electron flow). The coolant flow rate was set at 30 g/s, and an objective of 1000 K coolant outlet temperature was set. This problem is not symmetric about the converter midplane; however, it is desirable to match the voltage output from each end of the converter. As a first guess, the length of each converter section studied was set at 12.7 cm, the coolant temperature at midplane was set at 925 K, and current flow through the midplane was varied until the center voltages from the solution of each converter section matched. This solution provided insight into the selection of a second estimate of the boundary between left-side and right-side converters in order to match the output voltages of each side and into the second estimate of coolant temperature at the boundary plane. It was found that the voltage peaked some 0.6 cm to the outlet coolant temperature side of midplane, so the second estimate placed the boundary at 12.1 cm from the inlet end (i.e., converters of 12.1 and 13.3 cm in countercurrent electron flow were studied). The results of this iteration were quite close to a good final solution, as can be seen in Figs. 11 and 12. The net power from each side was closely matched and equal to 282 W.

D. Central Short

In this example, a central short in a 25.4-cm converter with leads at both ends was studied. To simplify matters the collector temperature was fixed at 1000 K. The symmetry of this problem allows the study of a 12.7-cm con-

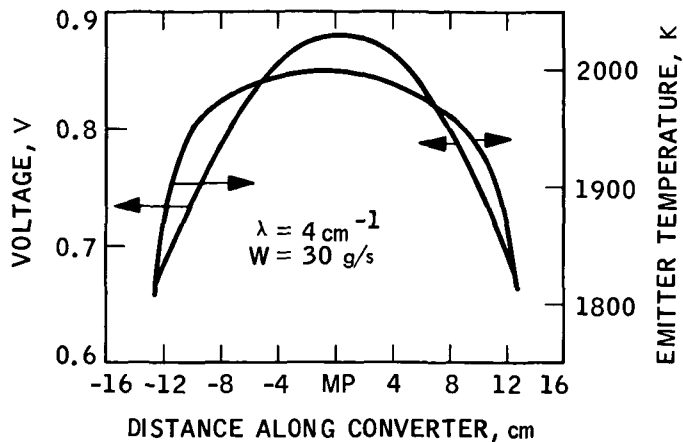


Fig. 11. Voltage and temperature profile for liquid metal cooled converter

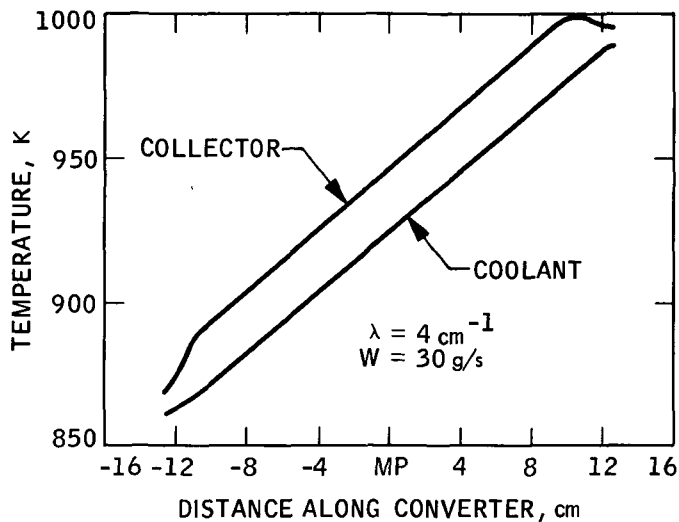


Fig. 12. Coolant and collector temperature profile for liquid metal cooled converter

verter. The normally operating converter characteristics are given in Section IV-A, where the output voltage and current correspond to a load resistance of 1.45 mΩ for the half-converter when $\lambda = 4 \text{ cm}^{-1}$.

The first case studied was that of short resistance equal to 0.725 mΩ (1.45 mΩ for the half-converter studied in symmetry). For a first estimate, the boundary between the two converters that must be studied to achieve a solution (central short creates symmetry, see Fig. 5) was set at 6.35 cm, i.e., one quarter of the 25.4-cm converter. The right-most converter, "d," (Fig. 5) is required to have a load resistance of 1.45 mΩ and a lead length-to-area ratio

λ of 4 cm^{-1} . The left converter, "c," has a short resistance of $1.45 \text{ m}\Omega$ computed from

$$R_s = \frac{v(l)}{i_e(l)} \quad (45)$$

and a short thermal conductance given by

$$\left(\frac{k}{\lambda}\right)_s = \frac{Q_e(l)}{(T_e(l) - T_c(l))} \quad (46)$$

Solution was obtained by varying $T_e(0)$ until the required right boundary conditions for converter "d" were obtained (Figs. 13 and 14). The short conductance obtained was 0.3 W/K . In order to vary the short conductance to any other desired value, the boundary between converters "c" and "d" would have to be varied.

To study an even lower short resistance, the next case arbitrarily moved the boundary between converters "c" and "d" to 9 cm from converter midplane; i.e., converter "c" was 9 cm long and converter "d" was 3.7 cm long. In this case, in addition to varying $T_e(0)$, it was also necessary to vary the current flow through the boundary $i_s(0)$ to achieve a voltage match between converters "c" and "d." Fortunately the matchup of the two converters is not sensitive to the choice of right boundary condition on converter "c" (the λ boundary condition in DEXTER) as can be seen in Figs. 15 and 16. This allowed a third plot in Figs. 13 and 14 at a value of (k/λ) , nearly the same as for the first short case to show the effect of varying short resistance only. For the short cases studied, Table 2 shows the net power and voltage obtainable from the converter as a function of short resistance.

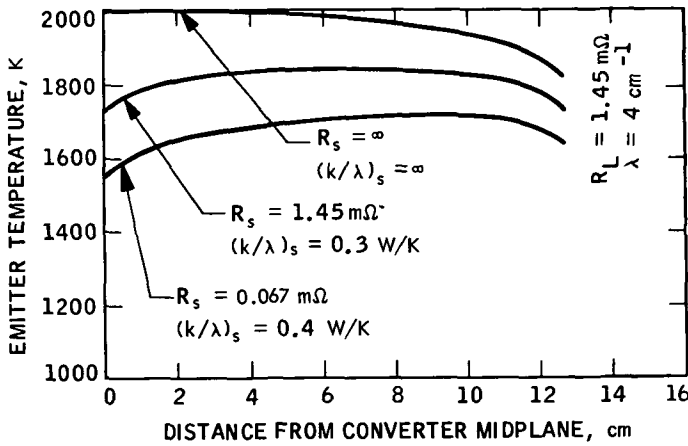


Fig. 13. Effect of central short on converter temperature profile

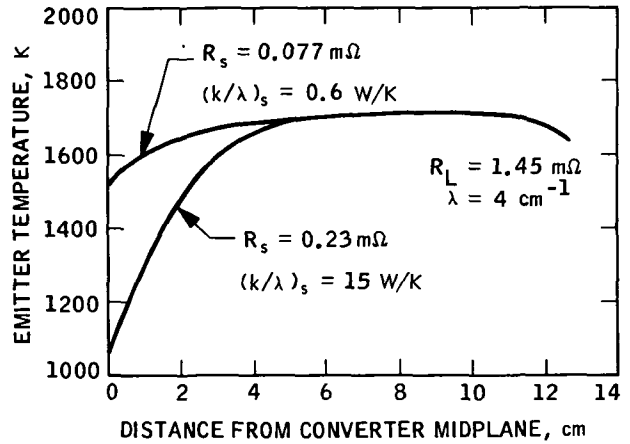


Fig. 15. Effect of varying short conditions on converter temperature profile

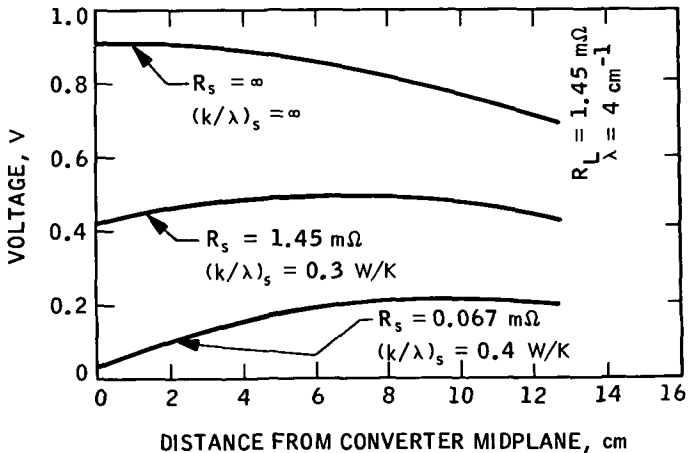


Fig. 14. Effect of central short on converter voltage profile

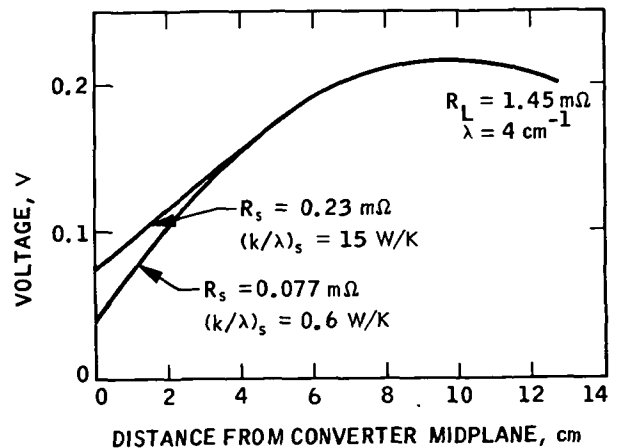


Fig. 16. Effect of varying short conditions on converter voltage profile

Table 2. Net performance of shorted converter

$R_s, m\Omega$	$(k/\lambda)_s, W/K$	P_{net}, W	v_{net}, V
∞	∞	294	0.62
1.45	0.3	105	0.39
0.067	0.4	24	0.18

values for each variable are included so that only desired changes need be made to execute the code. Table 3 lists the input data required by variable name and FORTRAN name and shows the built-in values.

V. User's Manual

Every attempt has been made to simplify the use of DEXTER. The input NAMELIST format and built-in

VI. Error Messages

Table 4 lists the current error messages and action taken.

Table 3. Input data for DEXTER

Variable name	FORTRAN name	Definition	Built-in value
ρ_s	RE1] RE2]	Coefficients in $\rho_s = RE1 + RE2 * T$	[$-1.203 \times 10^{-5} \Omega\text{-cm}$ [$3.445 \times 10^{-8} \Omega\text{-cm/K}$
k_s	TKE1] TKE2]	Coefficients in $k_s = TKE1 + TKE2 * T$	[1.33 W/cm-K [$-1.5 \times 10^{-4} \text{ W/cm-K}^2$
ρ_c	RC1] RC2]	Coefficients in $\rho_c = RC1 + RC2 * T$	[$6.0 \times 10^{-6} \Omega\text{-cm}$ [$3.77 \times 10^{-9} \Omega\text{-cm/K}$
k_c	TKC1] TKC2]	Coefficients in $k_c = TKC1 + TKC2 * T$	[0.472 W/cm-K [$1.127 \times 10^{-4} \text{ W/cm-K}$
ρ_{co}	RCOL1] RCOL2]	Coefficients in $\rho_{co} = RCOL1 + RCOL2 * T$	[$3.8 \times 10^{-6} \Omega\text{-cm}$ [$8.28 \times 10^{-9} \Omega\text{-cm/K}$
k_{co}	TKCOL1] TKCOL2]	Coefficients in $k_{co} = TKCOL1 + TKCOL2 * T$	[0.2154 W/cm-K [$7.667 \times 10^{-5} \text{ W/cm-K}^2$
d_{co}	DCOOL1] DCOOL2]	Coefficients in $d_{co} = DCOOL1 + DCOOL2 * T$	[0.943 g/cc [$-2.467 \times 10^{-4} \text{ g/cc-K}$
C_p	CPCOL1] CPCOL2]	Coefficients in $C_p = CPCOL1 + CPCOL2 * T$	[0.801 J/g K [$8.5 \times 10^{-5} \text{ J/g-K}^2$
k_L	TKLD1] TKLD2]	Coefficients in $k_L = TKLD1 + TKLD2 * T$	[1.33 W/cm-K [$-1.5 \times 10^{-4} \text{ W/cm-K}^2$
ρ_L	RL1] RL2]	Coefficients in $\rho_L = RL1 + RL2 * T$	[$-1.203 \times 10^{-5} \Omega\text{-cm}$ [$3.445 \times 10^{-8} \Omega\text{-cm/K}$
ϵ_s	EME1] EME2]	Coefficients in $\epsilon_s = EME1 + EME2 * T$	[0.026 [$1.168 \times 10^{-4}/K$
ϵ_c	EMC1] EMC2]	Coefficients in $\epsilon_c = EMC1 + EMC2 * T$	[0.0 [$1.11 \times 10^{-4}/K$
A_{s1}	AE1	See Nomenclature	2.29 cm^2
A_{s2}	AE2	See Nomenclature	2.29 cm^2
C_s	CE	See Nomenclature	4.39 cm
A_c	AC	See Nomenclature	0.9673 cm^2
C_c	CC	See Nomenclature	2.394 cm
A_{co}	ACOL	See Nomenclature	0 cm^2
λ	TEND	Desired value of λ for right boundary condition	4.0 cm^{-1}
D_{co}	DEQ	See Nomenclature	0.762 cm
l	ELDIOD	See Nomenclature	12.7 cm
d	DGAP	See Nomenclature	0.254 cm
T_{coo}	TCOLIN	See Nomenclature	1000 K
w	TCOLOT	See Nomenclature	30 g/s
T_{cs}	TCS	See Nomenclature	620 K
T_{co}	TEMAX	See Nomenclature	2000 K

Table 3 (contd)

Variable name	FORTRAN name	Definition	Built-in value
Q_{in}	PTH	Average value	40.0 W/cm ²
	P (10)	Unnormalized distribution function for Q_{in}	1.0
	PX (10)	Points at which function is specified	0.0 cm
	ANPX	Number of entries in P-PX tables	1.0
	XPLT (50)	Specified points for data printing	0.0, 1.0, 2.0, ..., 12.0, 12.7 cm
	ANP	Number of entries in XPLT table	14.0
$i_s(0)$; $i_c(0)$ for // flow	CURREN	Left boundary current	0.0 A
	ASAVE	Switch = 0. No effect = 1. VOLT, VU, VL input	0.0
$v(0)$	VOLT	Left boundary voltage guess	0.0 V
v_s	VU	See Nomenclature	0.0 V
v_L	VL	See Nomenclature	0.0 V
	DDV	If ASAVE = 0., VU = computed $v(0)$ (by Eq. 36) + DDV, VL = computed $v(0)$ - DDV	0.1 V
	COL	Switch = 0. Heat pipe cooled collector = 2. Liquid metal cooled converter	0.0
	AIT	Switch = 0. Want a data map vs λ = 1. Iterate to satisfy input TEND	0.0
	ACHT	Switch = 0. Switch not used	0.0
	AFLO	Switch = 0. Countercurrent electron flow = 1. Parallel electron flow	0.0
I_{sx}	CURE	See Nomenclature	0.0 A
I_{cx}	CURC	See Nomenclature	0.0 A

Table 4. Error messages in DEXTER

Message	Definition
SEAR 2	Unable to converge on desired right boundary condition (λ). $T_s(l)$, VOLT, VU, VL printed and case is terminated
SEARB	Unable to find a value of j which corresponds to desired v , T_s , T_c , and T_{cs} . T_s , T_c , j , T_{cs} , v , j_s , j_L printed and case is terminated
STEP SIZE TOO SMALL	Runge-Kutta failure in satisfying integration error criterion. Case is terminated
AVLO or ENTPL	Power distribution function not specified at $x = 0$. Problem terminated
AVHI or ENTPH	Power distribution function not specified at $x = l$. Problem terminated

Nomenclature

A_c	Collector cross-sectional area, cm^2	Q_{ec}	Electron cooling, W/cm^2
A_{e1}	Emitter cross-sectional area for electron flow, cm^2	Q_{in}	Input heat, W/cm^2
A_{e2}	Emitter cross-sectional area for heat flow, cm^2	Q_{rad}	Radiation heat transfer, W/cm^2
C_c	Collector surface area per unit length, cm	R_{cs}	Resistance of collector-collector short, Ω
C_e	Emitter surface area per unit length, cm	R_{es}	Resistance of emitter-emitter short, Ω
C_p	Coolant heat capacity, $\text{J}/\text{g}\cdot\text{K}$	R_l	Resistance of interconverter lead, Ω
D_{co}	Equivalent flow diameter for coolant, cm	R_L	Load resistance, Ω
d	Emitter-collector spacing, cm	R_s	Emitter-collector short resistance, Ω
h	Collector-coolant heat transfer coefficient, $\text{W}/\text{cm}^2\cdot\text{K}$	T_c	Collector temperature, K
I_{cs}	Excess (short) current flowing through collector, A	T_{co}	Coolant temperature, K
I_{es}	Excess (short) current flowing through emitter, A	T_{cs}	Cesium temperature, K
i_c	Collector current, A	T_e	Emitter temperature, K
i_e	Emitter current, A	T_L	Lead mean temperature, K
j	Thermionic current density, A/cm^2	v	Emitter-collector voltage, V
k_c	Collector thermal conductivity, $\text{W}/\text{cm}\cdot\text{K}$	v_L	Lower limit to $v(0)$, V
k_{co}	Coolant thermal conductivity, $\text{W}/\text{cm}\cdot\text{K}$	v_u	Upper limit to $v(0)$, V
k_e	Emitter thermal conductivity, $\text{W}/\text{cm}\cdot\text{K}$	w	Coolant flow rate, g/s
k_L	Lead thermal conductivity, $\text{W}/\text{cm}\cdot\text{K}$	x	Distance along converter, cm
l	Converter length from plane of zero heat flow, cm	ϵ_c	Collector emissivity
Q_c	Collector axial heat conduction, W	ϵ_e	Emitter emissivity
Q_{cs}	Cesium heat conduction, W/cm^2	λ	Lead length-to-area ratio, cm^{-1}
Q_e	Emitter axial heat conduction, W	ρ_c	Collector resistivity, $\Omega\cdot\text{cm}$
		ρ_{co}	Coolant resistivity, $\Omega\cdot\text{cm}$
		ρ_e	Emitter resistivity, $\Omega\cdot\text{cm}$
		ρ_L	Lead resistivity, $\Omega\cdot\text{cm}$
		σ	Stefan-Boltzmann constant, $\text{W}/\text{cm}^2\cdot\text{K}^4$

References

1. Davis, J. P., et al., "One-Dimensional Diode Heat Transfer Program Coupled to Thermionic Performance," Space Programs Summary 37-59, Vol. III, pp. 211-214. Jet Propulsion Laboratory, Pasadena, Calif., Oct. 31, 1969.
2. McCandless, R. J., and Hill, P. R., "Radiation Heat Transfer Calculations," in *1967 Thermionic Specialist Conversion Conference*, Palo Alto, Calif., Oct. 1967.
3. Kitrilakis, S., and Meeker, M., *J. Adv. Energy Conv.*, Vol. 3, pp. 59-68, 1963.
4. *Nuclear Engineering Handbook*, First Edition. Edited by H. H. Etherington, McGraw-Hill, New York, 1958.
5. Wilkins, D. R., *SIMCON*, GESR2109, General Electric Company, Pleasanton, Calif., 1968.

~~08976~~

N72-11207

TECHNICAL REPORT STANDARD TITLE PAGE

1. Report No. 32-1545	2. Government Accession No.	3. Recipient's Catalog No.	
4. Title and Subtitle DEXTER -- A ONE-DIMENSIONAL CODE FOR CALCULATING THERMIONIC PERFORMANCE OF LONG CONVERTERS		5. Report Date November 15, 1971	
		6. Performing Organization Code	
7. Author(s) C. D. Sawyer		8. Performing Organization Report No.	
9. Performing Organization Name and Address JET PROPULSION LABORATORY California Institute of Technology 4800 Oak Grove Drive Pasadena, California 91103		10. Work Unit No.	
		11. Contract or Grant No. NAS 7-100	
		13. Type of Report and Period Covered Technical Report	
12. Sponsoring Agency Name and Address NATIONAL AERONAUTICS AND SPACE ADMINISTRATION Washington, D.C. 20546		14. Sponsoring Agency Code	
		15. Supplementary Notes	
16. Abstract This report describes a versatile code for computing the coupled thermionic electric-thermal performance of long thermionic converters in which the temperature and voltage variations cannot be neglected. The code is capable of accounting for a variety of external electrical connection schemes, coolant flow paths and converter failures by partial shorting. Example problem solutions are included along with a user's manual.			
17. Key Words (Selected by Author(s)) Computer Programs Power Sources Thermionics		18. Distribution Statement Unclassified -- Unlimited	
19. Security Classif. (of this report) Unclassified	20. Security Classif. (of this page) Unclassified	21. No. of Pages 13	22. Price

HOW TO FILL OUT THE TECHNICAL REPORT STANDARD TITLE PAGE

Make items 1, 4, 5, 9, 12, and 13 agree with the corresponding information on the report cover. Use all capital letters for title (item 4). Leave items 2, 6, and 14 blank. Complete the remaining items as follows:

3. Recipient's Catalog No. Reserved for use by report recipients.
7. Author(s). Include corresponding information from the report cover. In addition, list the affiliation of an author if it differs from that of the performing organization.
8. Performing Organization Report No. Insert if performing organization wishes to assign this number.
10. Work Unit No. Use the agency-wide code (for example, 923-50-10-06-72), which uniquely identifies the work unit under which the work was authorized. Non-NASA performing organizations will leave this blank.
11. Insert the number of the contract or grant under which the report was prepared.
15. Supplementary Notes. Enter information not included elsewhere but useful, such as: Prepared in cooperation with... Translation of (or by)... Presented at conference of... To be published in...
16. Abstract. Include a brief (not to exceed 200 words) factual summary of the most significant information contained in the report. If possible, the abstract of a classified report should be unclassified. If the report contains a significant bibliography or literature survey, mention it here.
17. Key Words. Insert terms or short phrases selected by the author that identify the principal subjects covered in the report, and that are sufficiently specific and precise to be used for cataloging.
18. Distribution Statement. Enter one of the authorized statements used to denote releasability to the public or a limitation on dissemination for reasons other than security of defense information. Authorized statements are "Unclassified-Unlimited," "U. S. Government and Contractors only," "U. S. Government Agencies only," and "NASA and NASA Contractors only."
19. Security Classification (of report). NOTE: Reports carrying a security classification will require additional markings giving security and downgrading information as specified by the Security Requirements Checklist and the DoD Industrial Security Manual (DoD 5220.22-M).
20. Security Classification (of this page). NOTE: Because this page may be used in preparing announcements, bibliographies, and data-banks, it should be unclassified if possible. If a classification is required, indicate separately the classification of the title and the abstract by following these items with either "(U)" for unclassified, or "(C)" or "(S)" as applicable for classified items.
21. No. of Pages. Insert the number of pages.
22. Price. Insert the price set by the Clearinghouse for Federal Scientific and Technical Information or the Government Printing Office, if known.